Lifetime measurements of rubidium $nD_{3/2}$ ($n=6-9$) states using the Hanle effect

W. A. van Wijngaarden and J. Sagle
Department of Physics, York University, Toronto, Ontario, Canada M3J 1P3
(Received 17 June 1991; revised manuscript received 8 August 1991)

A Hanle experiment has been used to determine the following radiative lifetimes (in nsec) of rubidium: $\tau_{6D_{3/2}}=298\pm8$, $\tau_{7D_{3/2}}=345\pm9$, $\tau_{8D_{3/2}}=586\pm15$, and $\tau_{9D_{3/2}}=638\pm17$. These data were taken at a temperature of 293 K and are not corrected for effects due to blackbody radiation. The effect of the hyperfine interaction on the Hanle signal is discussed in detail for an excited state of arbitrary angular momentum.

PACS number(s): 32.70.Fw

I. INTRODUCTION

Accurate measurements of radiative lifetimes [1] can be used to test atomic theory. Alkali-metal atoms are especially attractive to model since all but one electron occupies a filled electronic shell. The interaction between the valence electron and the nucleus surrounded by the electron core, can be approximated by a hydrogenic potential [2]. This simple model has been refined [3] as a result of experiments that have revealed the effects of core polarization [4] and blackbody radiation [5], and uncovered small differences in the radiative lifetimes of states of the same fine-structure multiplet [6–8]. A comprehensive summary of theoretical and measured lifetime values has been given by Theodosiou [9]. In this paper we present the measurement of the radiative lifetimes for the $nD_{3/2}$ ($n=6-9$) states of rubidium using the Hanle effect [10–13].

The apparatus is schematically shown in Fig. 1. The atoms are excited by light propagating along the y direction and linearly polarized along the z axis. Low-lying excited states can be populated using lamps and continuous-wave lasers. To populate higher states, stepwise excitation or multiphoton excitation using pulsed lasers is required. The excitation is governed by the selection rule $\Delta m_z=0$, where m_z is the azimuthal quantum number measured with respect to the z axis. This is illustrated in Fig. 2(a) where an atom having an $S_{1/2}$ ground state is excited via a two-photon excitation to a

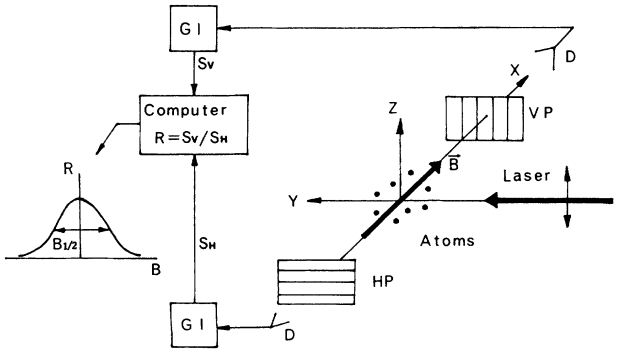

FIG. 1. Schematic experimental arrangement. The atoms are excited by a laser polarized along the z or vertical direction. Vertical (VP) and horizontal (HP) polarized fluorescence are detected by two detectors (D). The fluorescent signals are sent to gated integrators (GI) whose outputs are in turn input to a computer. The computer determines the ratio of the two signals S_V and S_H, and plots it as a function of the magnetic field B.

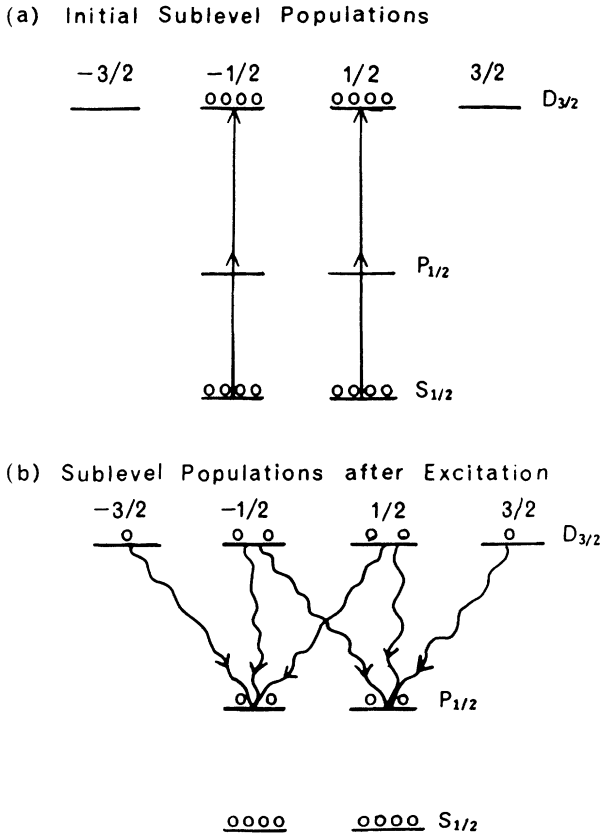

FIG. 2. Zeeman sublevel populations during experiment. Part (a) illustrates the population of the $m_J=\pm\frac{1}{2}$ sublevels of the $D_{3/2}$ state produced by a two-photon excitation of the ground state. In part (b), the atoms have been redistributed among the sublevels as a result of the Hanle field and the hyperfine interaction, as well as fluorescent decay to lower states such as $P_{1/2}$.

$D_{3/2}$ state. The excited state is perturbed by a magnetic field pointing in the x direction which transfers atoms among the Zeeman sublevels as shown in Fig. 2(b). The relative populations of the Zeeman sublevels can be monitored by detecting the fluorescence polarization when the excited state e radiatively decays to a lower state f. In this experiment, this time-decaying fluorescence is detected by a photomultiplier and integrated by a gated integrator. It is convenient to simultaneously monitor two fluorescence channels sensitive to orthogonal polarizations since the ratio of these two signals is independent of the excited-state number density. A computer then plots the ratio of the fluorescence fluences versus the magnetic field. This so-called Hanle signal, is a Lorentzian function for atoms having a negligible hyperfine interaction. The magnetic field width of this curve (full width at half maximum, FWHM) is proportional to the inverse of the excited-state lifetime. The hyperfine interaction complicates the signal by broadening the Hanle signal and generating additional peaks due to level crossings at higher magnetic fields [14]. We shall show how excited-state lifetimes can be determined using the Hanle effect when the hyperfine interaction is not negligible.

In this paper, Sec. II gives the theory for the general case where the states e and f have arbitrary angular momentum. Section III describes the apparatus and Sec. IV compares the results of this work to lifetimes found previously.

II. THEORY

Several accounts of the Hanle effect have been written that deal primarily with excitation of low-lying states not affected by the hyperfine interaction [11–13]. The following discussion uses the density matrix formalism that has been shown to be convenient in magnet-field-decoupling experiments to compute fluorescence-decay signals [15,16]. We consider an unpolarized atom that is excited at time $t=0$ to state e by light linearly polarized along the z direction. The initial state is described by the density matrix $\rho_e(0)$ which only has nonzero diagonal elements given as

$$\langle J_e m_z|\rho_e(0)|J_e m_z\rangle = A_0 + A_2 m_z^2 \ . \tag{1}$$

Here, J_e is the electronic angular momentum of state e and m_z is its azimuthal component measured along the z direction. A_0 and A_2 are constants satisfying the normalization condition $\mathrm{Tr}\rho_e(0)=1$. We next introduce the irreducible tensor operator [15]

$$T_{\mathrm{LM}}(J,J') = \sum_m |Jm\rangle\langle J'm-M|(-1)^{m-M-J} \times C(J,J',L;m,M-m) \ , \tag{2}$$

where the bra and ket vectors are quantized along the z axis and C is a Clebsch-Gordan coefficient. The initial excited-state density matrix then becomes

$$\rho_e(0) = \frac{1}{\sqrt{[J_e]}} T_{00}(J_e,J_e) + A T_{20}(J_e,J_e) \ , \tag{3}$$

where A is a linear combination of the constants A_0 and A_2.

The excited-state density matrix at time t is given by

$$\rho_e(t) = e^{-iHt/\hbar}\rho_e(0)e^{iHt/\hbar}e^{-t/\tau} \ . \tag{4}$$

Here, τ is the radiative lifetime of state e that we seek to determine and H is the Hamiltonian, which is given below.

$$H = H_0 + ah\mathbf{I}\cdot\mathbf{J} + bh\frac{[3(\mathbf{I}\cdot\mathbf{J})^2+\frac{3}{2}(\mathbf{I}\cdot\mathbf{J})-(\mathbf{I}\cdot\mathbf{I})(\mathbf{J}\cdot\mathbf{J})]}{2I(2I-1)J(2J-1)} + g_J\mu_B\mathbf{B}\cdot\mathbf{J} \ . \tag{5}$$

H_0 represents the Coulomb and fine structure. The next two terms are the magnetic dipole and electric quadrupole hyperfine interactions, whose magnitude depends on the nuclear spin $\mathbf{I}$ and on the coupling constants a and b. The final term describes the interaction of the electron with the external magnetic field $\mathbf{B}$, which points along the x direction. μ_B is the Bohr magneton and g_J is the Landé factor corresponding to the electronic angular momentum $\mathbf{J}$. The interaction of the magnetic field with the nucleus was ignored since it is negligibly small in this experiment.

The Hamiltonian mixes the populations of the excited state Zeeman sublevels $|J_e m_z\rangle$. This can be monitored by detecting the fluorescence emitted when state e radiatively decays to state f. A detector observes fluorescence linearly polarized along direction $\hat{\mathbf{u}}=(0,\sin\theta,\cos\theta)$ as shown in Fig. 3. The time-integrated fluorescent power or fluence is derived in Ref. [16] to be

$$S(B,\theta) = S_0 \sum_{ij} \frac{\langle i|\mathcal{L}|j\rangle\langle j|\rho_e(0)|i\rangle}{1+\omega_{ij}^2\tau^2} \ . \tag{6}$$

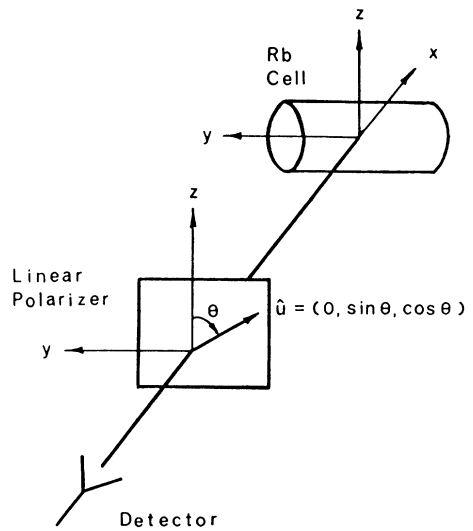

FIG. 3. Detection of linearly polarized fluorescence. Light is observed transverse to the laser propagation ($\hat{\mathbf{y}}$) and polarization ($\hat{\mathbf{z}}$) directions. The linear polarizer transmission axis is oriented along $\hat{\mathbf{u}}$.

S_0 is a constant proportional to various factors including the excited-state number density, the finite solid angle of the detector, and the transmission efficiency of various optical filters and polarizers. The state $|i\rangle$ is an eigenstate of the Hamiltonian corresponding to eigenenergy E_i and $\hbar\omega_{ij}=E_i-E_j$. In general, the eigenstates must be found numerically since no convenient set of basis states exists that simultaneously diagonalizes the hyperfine- and magnetic-field-interaction terms of the Hamiltonian. $\mathcal{L}$ is the fluorescent light operator which is given by

$$\mathcal{L}=\sum_L(-1)^L W(J_f,J_e,1,L;1,J_e)\times\sum_M(-1)^M U_{L-M}T_{LM}(J_e,J_e)\ . \tag{7}$$

W is a Racah coefficient and J_f is the angular momentum of state f. For detection of linearly polarized light, the nonzero U_{LM} are

$$\begin{aligned} U_{00}&=\frac{1}{\sqrt{3}}\ ,\\ U_{2\pm2}&=\frac{\sin^2\theta}{2}\ ,\\ U_{2\pm1}&=i\cos\theta\sin\theta\ ,\\ U_{20}&=\frac{1}{\sqrt{6}}(1-3\cos^2\theta)\ . \end{aligned} \tag{8}$$

The ratio of fluorescent fluences polarized parallel and perpendicular to the z axis is then

$$R(B)=\frac{S(B,0)}{S(B,\pi/2)}\ . \tag{9}$$

The ratio R, unlike the integrated signal S, is independent of the excited-state number density, which is difficult to measure. An analytic expression for R can be derived for an atom having negligible hyperfine interaction. The eigenstates of the Hamiltonian are then given by the Zeeman sublevels quantized along the magnetic field direction x, denoted by $|J_e m_x\}$. The sublevels quantized along the x and z directions are related by

$$|Jm_x\}=\sum_{m'}d^J_{m'm}(\pi/2)|Jm_z\rangle\ , \tag{10}$$

where $d^J_{m'm}$ is the rotation matrix element [17]. One then obtains the following result for the signal ratio,

$$R(B)=1+\frac{R_0}{1+(\omega\tau/\Theta)^2}\ , \tag{11}$$

where $\omega=g_J\mu_B B/\hbar$ is the Larmor frequency. $R(B)$ is a Lorentzian function having amplitude R_0 and angular half-width Θ which are given by

$$R_0=\frac{3x}{\sqrt{2}-x}\ , \tag{12}$$

$$\Theta=\left[\frac{\sqrt{2}-x}{4\sqrt{2}+2x}\right]^{1/2}\ , \tag{13}$$

where

$$x=-A\sqrt{[J_e]}\,\frac{W(J_f,J_e,1,2;1,J_e)}{W(J_f,J_e,1,0;1,J_e)}\ . \tag{14}$$

Figure 4(a) shows a plot of $R(B)$ that was computed using (11) for an atom, having a nucleus with spin 5/2, that is excited to a $D_{3/2}$ state as shown in Fig. 2, and radiatively decays to a $P_{1/2}$ level with a lifetime of 350 nsec.

It is useful to define a parameter $B_{1/2}$ to be the field where the ratioed signal given by (9) is halfway between the zero and high-field values denoted by $R(0)$ and $R(B_\infty)$ respectively; i.e.,

$$R(B_{1/2})=\frac{R(0)+R(B_\infty)}{2}\ . \tag{15}$$

The excited-state lifetime may then be found using

$$\tau=\frac{\Theta}{\omega_{1/2}}\ , \tag{16}$$

where $\omega_{1/2}=\omega(B_{1/2})$. Hence, the excited state lifetime τ can be determined by measuring the field half-width of the Hanle signal. This measurement is relatively insensitive to factors affecting the signal amplitude such as the finite solid angle of the detector or the relative efficiency of the detectors measuring vertically and horizontally polarized fluorescence.

The hyperfine interaction perturbs the Hanle signal most significantly when the magnetic field is zero. The Hamiltonian eigenstates are then $|JIFm_F\rangle$, where $\mathbf{F}=\mathbf{J}+\mathbf{I}$ and m_F is the corresponding azimuthal quantum number. The signal ratio is then given by

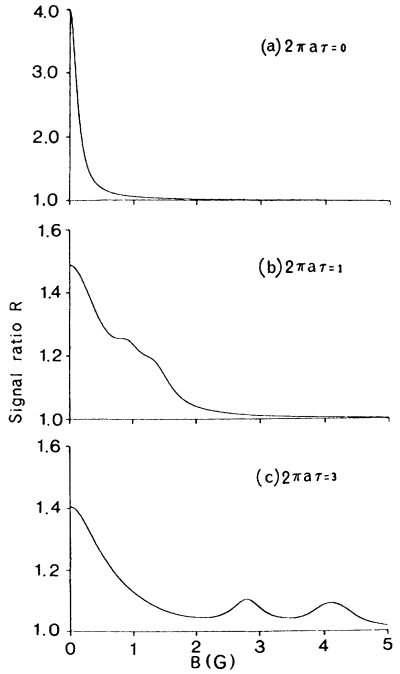

FIG. 4. Effect of hyperfine interaction $a\mathbf{I}\cdot\mathbf{J}$ on signal ratio. The signals are computed for atoms, having a nucleus of spin 5/2, that are excited to a $D_{3/2}$ state as shown in Fig. 2, and radiatively decay to a $P_{1/2}$ level with a lifetime of 350 nsec.

$$R(0)=\frac{1+\sqrt{2}\,xy}{1-xy/\sqrt{2}}\ , \tag{17}$$

where

$$y=\frac{1}{[I]}\left[2\sum_{F<F'}\frac{[F][F']W^2(I,F,J_e,2;J_e,F')}{1+\omega_{FF'}^2\tau^2}+\sum_{F}[F]^2W^2(I,F,J_e,2;J_e,F)\right]. \tag{18}$$

When the hyperfine interaction is negligible, the factor y is unity and the signal ratio given by (17) agrees with that predicted by Eqs. (11) and (12). Figure 4 illustrates the effect of the hyperfine interaction on the signal ratio for the simple case where only the magnetic-dipole term contributes to the hyperfine interaction. The strength of the hyperfine interaction is then characterized by a dimensionless constant that equals the product of the hyperfine frequency $\omega_{FF'}\approx 2\pi a$ times the excited-state lifetime τ. The factor y reduces the Hanle signal amplitude, and thereby increases the field halfwidth $B_{1/2}$. When $2\pi a\tau$ equals unity, additional peaks appear due to high-field level crossings [14]. The level-crossing peaks move out to higher magnetic fields as the magnetic dipole constant increases further and become well separated from the so-called zero field or Hanle signal as is illustrated in Fig. 4(c). The dependence of the parameter Θ on the hyperfine interaction is shown in Fig. 5. This graph was generated by first determining $B_{1/2}$ from Fig. 4 and then using Eq. (16). When $2\pi a\tau\approx\omega_{FF'}\tau<1$, Θ is especially sensitive to the hyperfine interaction.

In this experiment, the lifetime was determined as follows. First, the known values of the magnetic dipole and electric quadrupole hyperfine constants a and b were used to generate a table listing τ versus computed Θ or $B_{1/2}$ values. For the states considered in this experiment $\omega_{FF'}\tau>3$ and Θ could be evaluated to an accuracy of 1%. The lifetime was then found using the value of $B_{1/2}$ measured from the experimental data.

The zero-field level crossing or Hanle signal can be approximated by a Lorentzian function as is shown in Fig. 6. The Lorentzian curve was chosen to have the same halfwidth as determined by (15) for the computed signal, and have zero- and high-field values found using (17) and (11). Very close agreement between the exact and fitted curves is obtained if the high-field level-crossing peaks are well separated from the zero-field or Hanle signal. In our experiment, data analysis was expedited by fitting a Lorentzian function to the experimentally measured data points. We estimate the error in equating $B_{1/2}$ to the half-width at half maximum of the Lorentzian curve to be about 2%.

III. EXPERIMENT

A. Apparatus and procedure

We shall present a brief description of the apparatus emphasizing aspects relevant to lifetime measurements. Detailed discussions about laser excitation of atoms stored in a cell and about fluorescence detection are given elsewhere [16]. Rubidium atoms were contained in a cylindrical pyrex cell having a length of 10 in. and a diameter of 1 in. The cell was evacuated by a diffusion pump to a pressure of 1×10^{-7} Torr before it was filled with rubidium. Simultaneously, it was baked overnight at a temperature of several hundred degrees centigrade to remove impurities. The cell was located in an oven heated by jets of hot air to a temperature of 120 °C. This corresponds to a rubidium number density of 2.0×10^{13} atoms/cm^3 [18]. Hence, the probability of a collision between an excited rubidium atom and either a background gas molecule or with the cell wall is negligible.

The magnetic field was controlled using three pairs of orthogonal Helmholtz coils centered about the cell. The

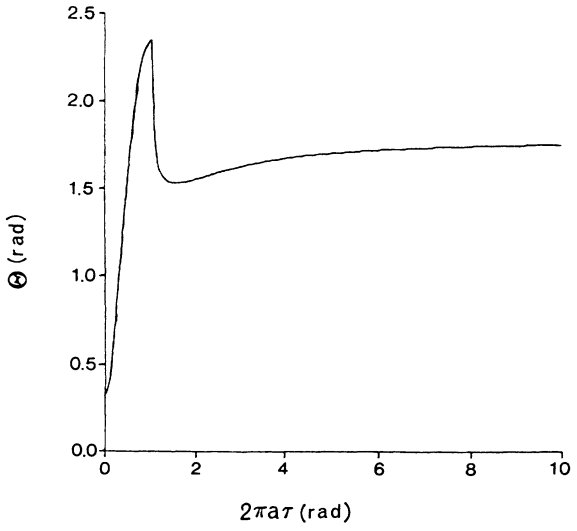

FIG. 5. Effect of hyperfine interaction on Θ.

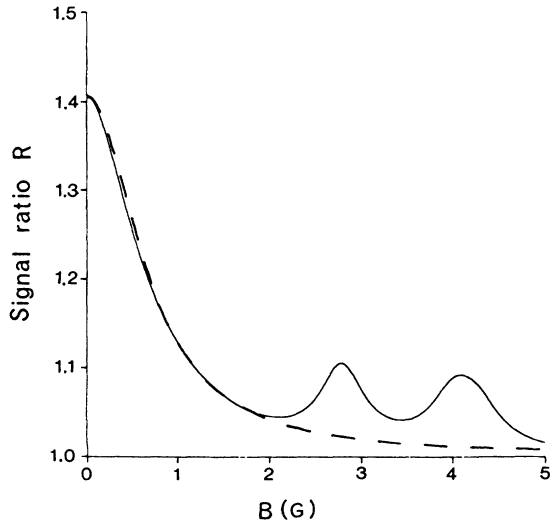

FIG. 6. Lorentzian fit to computed signal ratio. The solid line is the same signal ratio R as appears in Fig. 4(c). The dashed curve is a Lorentzian function that was fit to the exact signal as is described in the text.

Hanle field in the x direction was determined using a Hall-effect gaussmeter to an accuracy of 1%. This uncertainty greatly exceeded the field inhomogeneity over the region of the cell from which fluorescence was detected. The field components along the y and z axes were measured to be less than 5 mG.

A pulsed dye laser excited the $5S_{1/2}$ rubidium ground state to the $nD_{3/2}$ $n=(6-9)$ state via a two-photon excitation. Typical laser-pulse energies were between 1 and 10 mJ. Fluorescence produced by the decay of the $D_{3/2}$ state to the $5P_{1/2}$ level was detected using a narrow-band interference filter (FWHM of 10 Å) and a photomultiplier (Hamamatsu R928). The time decaying photomultiplier signal was integrated (Stanford Research Systems 250) and sent to a computer. The ratio of signals obtained with the polarizer in front of the detector oriented along the vertical and horizontal directions was then evaluated and plotted versus the magnetic field.

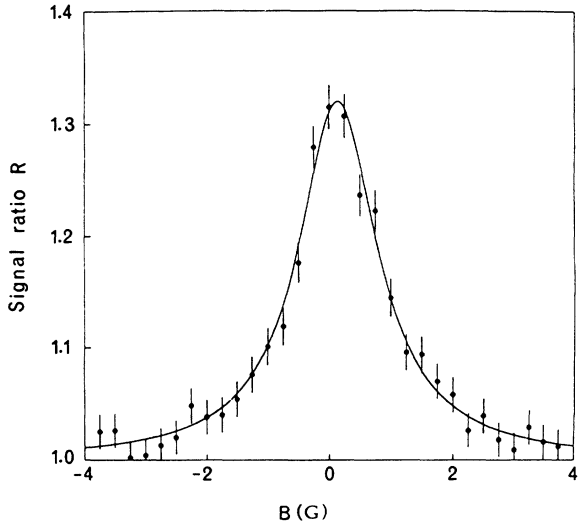

FIG. 7. Sample of experimental data. A Lorentzian function was fit to the data using a least-square fitting program.

B. Data analysis

A measured Hanle signal is shown in Fig. 7, for the case where the $6D_{3/2}$ state was excited. The following Lorentzian function was fit to the data,

$$F(B)=1+\frac{F_0}{1+[(B-B_0)/B_{1/2}]^2}\ , \tag{19}$$

where F_0, B_0, and $B_{1/2}$ were varied using a least-squares algorithm to find the best fit. $B_{1/2}$ was then set equal to the average of the best-fit half-width values obtained for the separate runs. The uncertainty in $B_{1/2}$ is set equal to one standard deviation of the best-fit halfwidths about their average value. The Lorentzian is offset from the origin by B_0, which cancels the component of the Earth's field along the x direction. B_0 was found to be 0.10 G. The observed signal amplitude value, $F_0=0.32$, is lower than the value 0.40 which is predicted using (17) and (18) for the $nD_{3/2}$ ($n=6-9$) states of Rb^{85}. This means that more horizontal polarized fluorescence was detected than expected. It has been previously suggested that this might occur if the $\pm 3/2$ Zeeman sublevels are initially populated [16]. We therefore studied how different initial states described by the following density matrix affect the Hanle signal.

$$\rho_e(0)=\frac{1}{2(1+\alpha)}(\alpha|3/2\rangle\langle 3/2|+|1/2\rangle\langle 1/2|+|-1/2\rangle\langle -1/2|+\alpha|-3/2\rangle\langle -3/2|)\ . \tag{20}$$

The parameter α is zero for the case of a two-photon excitation from an $S_{1/2}$ to a $D_{3/2}$ state generated by a laser linearly polarized along the quantization axis. The Hanle curves were computed and are shown in Fig. 8. The signal amplitude decreases rapidly as α increases. It equals zero when all the sublevels are equally populated (i.e., $\alpha=1$). However, the field half-width shown in Fig. 9 changes less than 1% as α increases from 0.0 to 0.4. Therefore, the magnetic field width of the Hanle signal is relatively insensitive to the precise composition of the initial state and α was set to zero when analyzing the data.

IV. RESULTS

The lifetimes found for the $nD_{3/2}$ ($n=6-9$) states of rubidium are listed in Table I, along with the respective

TABLE I. Measured lifetimes.

	Hyperfine constants		Lifetimes (nsec)				
			This work	Ref. [24]		Ref. [26]	Refs. [19 and 20]
State	a (MHz)	b (MHz)	393 K	350 K	Ref. [25]	520 K	393 K
$6D_{3/2}$	2.32±0.06[a]	1.62±0.06[a]	298±8	285±16	294±12		254±27
$7D_{3/2}$	1.415±0.03[b]	0.31±0.06[b]	345±9	388±25	370±25		346±25
$8D_{3/2}$	0.84±0.01[c]	0.0	586±15	515±30			
$9D_{3/2}$	0.55[d]	0.0	638±17			565±120	

[a]Reference [19].
[b]Reference [20].
[c]Reference [21].
[d]Reference [22].

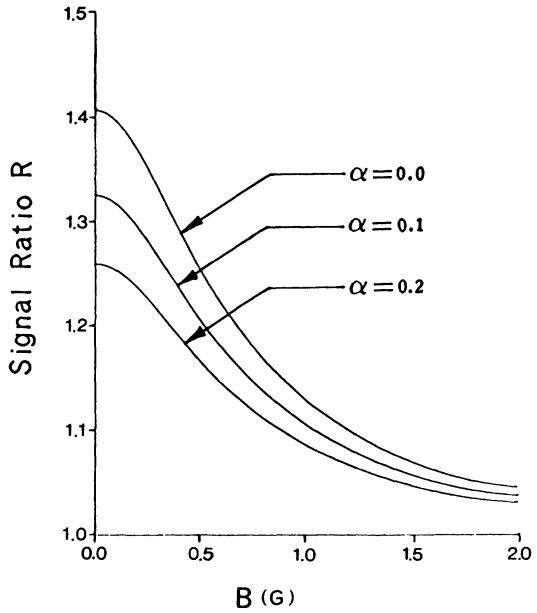

FIG. 8. Effect of initial state on signal ratio. The Hanle signals were computed for an initial state described by (20). α measures the fraction of atoms initially excited into the $\pm 3/2$ sublevels of a $D_{3/2}$ state. The curve computed when $\alpha=0.0$ is the same as that shown in Fig. 4(c).

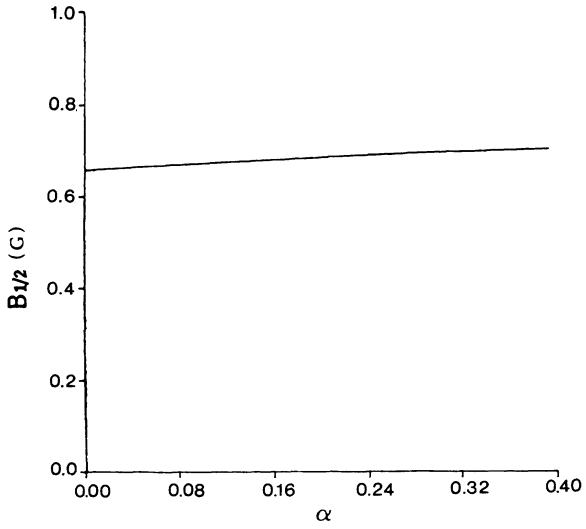

FIG. 9. Effect of initial state on magnetic-field half-width. The magnetic field half-widths $B_{1/2}$ of the Hanle signals shown in Fig. 8 were determined and plotted vs α.

magnetic dipole and electric quadrupole constants [19-22]. The hyperfine constants were determined by quantum beats and level-crossing experiments which have been described by Arimondo *et al.* [23]. The quoted lifetime error is determined by the uncertainty in $B_{1/2}$. Table I includes other measurements of the $D_{3/2}$ lifetimes, showing reasonable agreement with those obtained using the Hanle method [19,20,24–27]. The other experiments all determined the lifetime from the temporal dependence of the fluorescent intensity emitted when the excited-state radiatively decays. The temperatures at which the data were taken are also given, since none of the lifetimes have been corrected for blackbody radiation. This effect can cause significant depletion of high-lying-excited-state populations at room temperature [5].

Theoretical values for the lifetimes are listed in Table II. Decay rates have been computed using a Coulomb approximation as was first done by Bates and Damgaard [2]. We show the results of Gruzdev and Denisov [28], who accounted for the contribution of the polarized core to the transition dipole operator as is described by Curtis [4]. Lifetimes have also been computed using a numerical Coulomb approximation introduced by Lindgard and Nielsen [29]. The values found by the above authors are in close agreement. Neither Gruzdev and Denisov nor Lindgard and Nielsen take into account the spin-orbit interaction or blackbody radiation. This has been carefully done by Theodosiou [9], who computed lifetimes at the temperatures shown in Table I. At 0 K, his results are about 15% lower than those computed by the other two groups. The measured lifetimes exceed the values found by Theodosiou by a similar amount.

A comparison of the Hanle method to that measuring the exponential decay of fluorescence intensity has been made by Bulos *et al.* [13]. The Hanle method uses a box-car integrator rather than a relatively expensive transient digitizer. The magnetic fields needed to measure lifetimes as short as 1 ns are readily obtained using air-cooled Helmholtz coils. For both methods, data analysis is straightforward since either a Lorentzian or an exponential function is fit to the data. However, extraction of the lifetime from the Hanle signal requires accurate values of the hyperfine constants of the excited state. Fortunately, for many excited states these constants have been measured to accuracies of better than 1% [23]. In con-

TABLE II. Theoretical lifetimes (nsec).

State	Theodosiou [Ref. 9] 0 K	Theodosiou [Ref. 9] 350 K	Theodosiou [Ref. 9] 450 K	Lindgard and Nielsen [Ref. 29]	Gruzdev and Denisov [Ref. 28]
$6D_{3/2}$	253.62	251.32	248.60	295.1	300
$7D_{3/2}$	331.08	323.65	318.01	386.5	400
$8D_{3/2}$	455.48	438.01	427.86	532.4	560
$9D_{3/2}$	625.98	591.42	574.65	722.8	750

clusion, we believe the Hanle method is a useful tool for accurately measuring radiative lifetimes. Lifetimes were determined for the $nD_{3/2}$ ($n=6-9$) states of rubidium and were found to be in reasonable agreement with those calculated using a Coulomb approximation that takes into account polarization of the core electrons.

ACKNOWLEDGMENTS

This work was supported by the Natural Sciences and Engineering Research Council of Canada and by York University. We would like to thank Jian Li for technical assistance and the Ontario Laser and Lightwave Centre for the loan of equipment.

[1] J. R. Fuhr, B. J. Miller, and G. A. Martin, in *Bibliography on Atomic Transition Probability, 1914 Through October 1977,* Nat. Bur. Stand. (U.S.) Spec. Pub. No. 505 and supplements (U.S. GPO, Washington, D.C., 1978).

[2] D. R. Bates and A. Damgaard, Philos. Trans. R. Soc. London **242**, 101 (1949).

[3] I. Lindgren and J. Morrison, *Atomic Many-Body Theory* (Springer-Verlag, New York, 1986).

[4] L. J. Curtis, J. Phys. B **12**, L509 (1979).

[5] T. F. Gallagher and W. E. Cooke, Phys. Rev. Lett. **42**, 835 (1979).

[6] W. S. Neil and J. B. Atkinson, J. Phys. B **17**, 693 (1984).

[7] J. Carlsson and L. Sturesson, Z. Phys. D **14**, 281 (1989).

[8] A. Gaupp, P. Kuske, and H. J. Andra, Phys. Rev. A **26**, 3351 (1982).

[9] C. Theodosiou, Phys. Rev. A **30**, 2881 (1984).

[10] W. Hanle, Z. Phys. **30**, 93 (1924).

[11] W. Happer, *Beam-Foil Spectroscopy* (Gordon and Breach, New York, 1968), p. 305.

[12] A Corney, *Atomic and Laser Spectroscopy* (Clarendon, Oxford, 1977).

[13] B. R. Bulos, R. Gupta, and W. Happer, J. Opt. Soc. Am. **66**, 426 (1976).

[14] S. Svanberg, P. Tsekeris, and W. Happer, Phys. Rev. Lett. **30**, 817 (1973).

[15] R. Gupta, S. Svanberg, and W. Happer, Phys. Rev. A **6**, 529 (1972).

[16] W. A. van Wijngaarden and J. Sagle, Phys. Rev. A **43**, 2171 (1991).

[17] M. E. Rose, *Elementary Theory of Angular Momentum* (Wiley, New York, 1963).

[18] A. N. Nesmeianov, *Vapor Pressure of The Elements* (Academic, New York, 1963).

[19] W. A. van Wijngaarden, K. D. Bonin, and W. Happer, Phys. Rev. A **33**, 77 (1986).

[20] W. A. van Wijngaarden and J. Sagle, J. Phys. B **24**, 897 (1991).

[21] W. Hogervorst and S. Svanberg, Phys. Scr. **12**, 67 (1975).

[22] $a_9D_{3/2}$ was found from the data for the $(6-8)D_{3/2}$ states using the scaling law $a \propto n^{-3}$ where n is the effective principal quantum number.

[23] E. Arimondo, M. Inguscio, and P. Violino, Rev. Mod. Phys. **49**, 31 (1977).

[24] H. Lundberg and S. Svanberg, Phys. Lett. **56A**, 31, (1976).

[25] A. Ya Nikolaich and A. L. Osherovich, Vestn. Leningr. Univ. Fiz. Khim. **2**, 44 (1976).

[26] F. Gounand, M. Hugon, and P. R. Fournier, J. Phys. (Paris) **41**, 119 (1980).

[27] Table I does not include lifetimes measured by the following two experiments that did not resolve the fine-structure splitting of the nD states. J. Marek and P. Munster, J. Phys. B **13**, 1731 (1980); G. Waligorski, P. Kowalczyk, and C. Radzewicz, Z. Phys. D **3**, 79 (1986).

[28] P. F. Gruzdev and V. I. Denisov, Opt Spektrosk. **52**, 15 (1982) [Opt. Spectrosc. (USSR) **52**, 8 (1982)].

[29] A. Lindgard and S. E. Nielsen, At. Data Nucl. Data Tables **19**, 533 (1977).